

---

# Time-Variant Variational Transfer for Value Functions

---

**Giuseppe Canonaco\***

Politecnico di Milano, Milan, Italy  
giuseppe.canonaco@polimi.it

**Andrea Soprani\***

Politecnico di Milano, Milan, Italy  
andrea.soprani96@gmail.com

**Manuel Roveri**

Politecnico di Milano, Milan, Italy  
manuel.roveri@polimi.it

**Marcello Restelli**

Politecnico di Milano, Milan, Italy  
marcello.restelli@polimi.it

## Abstract

In most transfer learning approaches to reinforcement learning (RL) the distribution over the tasks is assumed to be stationary. Therefore, the target and source tasks are i.i.d. samples of the same distribution. In the context of this work, we will consider the problem of transferring value functions through a variational method when the distribution generating the tasks is time-variant, proposing a solution leveraging this temporal structure inherent to the task generating process. Moreover, by means of a finite sample analysis, the previously mentioned solution will be theoretically compared to its time-invariant version. Finally, we will provide an experimental evaluation of the proposed technique with three distinct time dynamics in three different RL environments.

## 1 Introduction

The reinforcement learning (RL) framework [30] is becoming increasingly more effective in dealing with complex problems [37, 29, 25] at the cost of requiring a huge amount of experience in order to achieve these impressive results. Therefore, a desirable feature for RL algorithms is sample efficiency, which could be reached, among all other alternatives, through transfer learning (TL) [32, 16]. TL allows an RL algorithm to reuse knowledge coming from a set of already solved tasks in order to speed up the learning phase of new ones. Depending on what kind of knowledge representation is being transferred, we have different TL algorithms in the related literature. Therefore, in order to perform transfer, we could have algorithms leveraging policies or options [8, 15], samples [31, 18, 36, 34], features [2, 19], value-functions [33, 35] or parameters [13, 1, 24, 7].

In the classical TL setting, the source and target tasks usually come from the same distribution, hence it would be sensible to use the Bayesian framework in order to iteratively refine the prior knowledge coming from the source tasks as more evidence from the target is collected. Following this rationale, in [38], under the assumption that the tasks share similarities in their Markov Decision Process (MDP) [27] representation, a hierarchical Bayesian solution is proposed, whose main drawback lies within the need to solve an auxiliary MDP in order to perform actions on the current task being tackled. Another methodology, along this line of research, has been developed in [17], which still leverages hierarchical Bayesian models, but this time assuming the tasks share commonalities through their value functions. Furthermore, in [6], a Bayesian framework able to adapt optimal policies to variations of the task dynamics is developed. They use a latent variable, which together with the state-action couple entirely describe the system dynamics. The uncertainty over the latent

---

\*equal contribution

variable is modeled independently of the uncertainty over the state, this limitation is overcome in the extension to their framework proposed in [13]. In [26] another extension to [6] is proposed, which accounts for multiple factors of variation potentially coming also from the reward function. A more general and efficient approach is developed, instead, in [35], which iteratively refines the distribution over optimal value functions by means of a variational procedure as more experience from the target task is collected.

In real-world applications it is highly likely that the system to be controlled by an agent evolve with time. Therefore, in the task generating process of a family of similar tasks there could be an underlying time dynamic to be accounted for. Time dynamics are usually not considered in the related TL literature. For this reason, in this paper, we will extend the work developed in [35] in order to take into account a time-variant distribution inherent to the task generating process. We will, then, provide a theoretical comparison between our solution and the time-invariant approach of [35]. Finally, we will provide an experimental comparison of the two approaches in three different RL environments with three distinct time dynamics.

## 2 Preliminaries

In this section, we describe the setting introduced in [35] adding a time-variant distribution over the tasks. We will start with basic RL concepts and some notation in Section 2.1, and we will conclude with the variational approach to transfer in Section 2.2.

### 2.1 Reinforcement Learning Background

Let us consider a time-variant distribution  $\mathcal{D}$  over tasks. We model each task  $\mathcal{M}_i$  coming from  $\mathcal{D}$  as a discounted Markov Decision Process (MDP) [27], which is defined as a tuple  $\mathcal{M}_i = \{\mathcal{S}, \mathcal{A}, \mathcal{P}_i, \mathcal{R}_i, p_0, \gamma\}$ .  $\mathcal{S}$  and  $\mathcal{A}$  represent the state space and the action space, respectively.  $\mathcal{P}_i$  is the Markovian transition function, where  $\mathcal{P}_i(s'|s, a)$  is the transition density from state  $s$  to state  $s'$  given that the action  $a$  is executed on the environment.  $\mathcal{R}_i : \mathcal{S} \times \mathcal{A} \rightarrow \mathbb{R}$  is the reward function, assumed to be uniformly bounded by a constant  $R_{max} > 0$ .  $p_0$  and  $\gamma \in [0, 1)$  are the initial state distribution and the discount factor, respectively. Therefore, for each task  $i$  our goal is to find a deterministic policy,  $\pi_i : \mathcal{S} \rightarrow \mathcal{A}$ , maximizing the long-term return over a possibly infinite horizon. In other words, this means being able to get  $\pi_i^* \in \arg \max_{\pi_i} J_i(\pi_i)$ , where  $J_i(\pi_i) = \mathbb{E}_{\mathcal{M}_i, \pi_i} [\sum_{t=0}^{\infty} \gamma^t \mathcal{R}_i(s_t, a_t)]$ . The optimal policy  $\pi_i^*$  is a greedy policy w.r.t. the optimal value function, i.e.,  $\pi_i^*(s) = \arg \max_a Q_i^*(s, a)$  for all  $s$ , where  $Q_i^*(s, a)$  is defined as the expected return obtained by taking action  $a$  in state  $s$  and then following the optimal policy afterward. From now on, for the sake of readability, we drop the  $i$  subscript whenever this does not imply ambiguity.

In this context, we focus on a set of parametrized value functions,  $\mathcal{Q} = \{Q_\theta : \mathcal{S} \times \mathcal{A} \rightarrow \mathbb{R} | \theta \in \mathbb{R}^p\}$ , also called  $Q$ -functions. We assume that each  $Q_\theta \in \mathcal{Q}$  is uniformly bounded by  $\frac{R_{max}}{1-\gamma}$ . An optimal  $Q$ -function is also the fixed point of the optimal Bellman operator [27], which is defined as follows:  $TQ_\theta(s, a) = \mathcal{R}(s, a) + \gamma \mathbb{E}_{s' \sim \mathcal{P}} [\max_{a'} Q_\theta(s', a')]$ . Therefore, a measure of optimality for a value function during learning is its Bellman error, defined as  $B_\theta = TQ_\theta - Q_\theta$ . Of course, if  $B_\theta(s, a) = 0 \forall (s, a) \in \mathcal{S} \times \mathcal{A}$ , then  $Q_\theta$  is optimal, which implies that minimizing the squared Bellman error,  $\|B_\theta\|_\nu^2$ , is a good objective for learning ( $\nu$  is the distribution over  $\mathcal{S} \times \mathcal{A}$ , assumed to exist). In practice, the Bellman error is not used, since it requires two independent samples of the next state  $s'$  for each couple  $(s, a)$  [20, 30]. For this reason, usually, the Bellman error is replaced by the Temporal Difference (TD) error  $b(\theta)$ , which correspond to an approximation of the former using one sample  $\langle s_h, a_h, r_h, s_{h+1} \rangle$ , so  $b_h(\theta) = r_h + \gamma \max_{a'} Q_\theta(s_{h+1}, a') - Q_\theta(s_h, a_h)$ . Therefore, given a set  $D = \langle s_h, a_h, r_h, s_{h+1} \rangle_{h=1}^N$  the squared TD error is  $\|B_\theta\|_D^2 = \frac{1}{N} \sum_{h=1}^N b_h(\theta)^2$ .

### 2.2 Variational Transfer of Value Functions

In the previously described context, an optimal solution to an RL problem is a greedy policy w.r.t. an optimal value function that is parametrized by a vector of weights  $\theta$ . Therefore, we can safely consider a distribution over optimal weights  $p(\theta)$  instead of the distribution  $\mathcal{D}$  over tasks since the latter induces a distribution over optimal  $Q$ -functions [35]. Now, given a prior on the weights  $p(\theta)$  and a dataset  $D = \langle s_h, a_h, r_h, s_{h+1} \rangle_{h=1}^N$ , the optimal Gibbs posterior minimizing an oracle upper

---

**Algorithm 1** Variational Transfer

---

```

1: Input: Target task  $\mathcal{M}_i$ , source weights  $\Theta_s$ 
2: Estimate prior  $p(\theta)$  from  $\Theta_s$ 
3: Initialize parameters:  $\xi \leftarrow \arg \min_{\xi \in \Xi} D_{KL}(q_\xi || p)$ 
4: Initialize dataset  $D = \emptyset$ 
5: while True do
6:   Sample initial state  $s_0 \sim p_0$ 
7:   while  $s_h$  is not terminal do
8:     Sample weights  $\theta \sim q_\xi(\theta)$ 
9:     Take action  $a_h = \arg \max_a Q_\theta(s_h, a)$ 
10:     $s_{h+1} \sim \mathcal{P}_i(\cdot | s_h, a_h)$ ,  $r_{h+1} = \mathcal{R}_i(s_h, a_h)$ 
11:     $D \leftarrow D \cup \langle s_h, a_h, r_{h+1}, s_{h+1} \rangle$ 
12:    Estimate  $\nabla_\xi \mathcal{L}(\xi)$  using  $D' \subseteq D$ 
13:    Update  $\xi$  with  $\nabla_\xi \mathcal{L}(\xi)$  using any optimizer
14:   end while
15: end while

```

---

bound on the expected loss is known to be [4]:

$$q(\theta) = \frac{e^{-\Psi \|B_\theta\|_D^2} p(\theta)}{\int e^{-\Psi \|B_{\theta'}\|_D^2} p(\theta') d\theta'}, \quad (1)$$

where  $\Psi > 0$ , which will be set to  $\psi^{-1}N$ , for some constant  $\psi > 0$  as in [35]. It is worth noticing that  $q$  becomes a Bayesian posterior every time  $e^{-\Psi \|B_\theta\|_D^2}$  can be interpreted as the likelihood of  $D$ . Since the integral at the denominator of Equation (1) is intractable, a variational approximation through a parametrized family of posteriors  $q_\xi$ , such that  $\xi \in \Xi$ , is proposed. In this way, it is sufficient to find  $\xi^*$  such that  $q_{\xi^*}$  minimizes the Kullback-Leibler (KL) divergence w.r.t. the Gibbs posterior  $q$ , which is equivalent to minimize the (negative) evidence lower bound (ELBO) [3]:

$$\min_{\xi \in \Xi} \mathcal{L}(\xi) = \min_{\xi \in \Xi} \left\{ \mathbb{E}_{\theta \sim q_\xi} [\|B_\theta\|_D^2] + \frac{\psi}{N} D_{KL}(q_\xi(\theta) || p(\theta)) \right\}. \quad (2)$$

Therefore, the idea behind the variational transfer of value functions (Algorithm 1) is to alternate a sampling from the posterior on the optimal value function with the optimization of the posterior via  $\nabla_\xi \mathcal{L}(\xi)$ , assuming to have already solved a finite number of source tasks  $\mathcal{M}_1 \dots \mathcal{M}_n$ , which, in turn, implies having the set of their approximate solutions  $\Theta_s = \{\theta_1, \dots, \theta_n\}$ . The weight resampling can be interpreted as a guess on the task we need to solve based on the current belief. After the sampling, the algorithm acts on the RL problem as if such guess were correct and then will adjust the belief based on the collected new experience through the optimization of the variational parameters  $\xi$ . Notice that, as long as  $\nabla_\xi \mathcal{L}(\xi)$  can be efficiently computed, any approximator for the  $Q$ -functions and any prior/posterior distributions can be used. To this end, since the *max* operator in the temporal difference error of Equation (2) is not differentiable, the *mellowmax* is used instead, which is differentiable and was proven to converge to the same fixed point of the optimal Bellman operator in [35]. From now on, we denote the mellow Bellman error with  $\tilde{B}_\theta$ .

### 3 Time-Variant Kernel Density Estimation for Variational Transfer

In the context of this work, we will model the evolution of time over a discrete grid of asymptotically dense time instants. Let  $\{\theta_{ij}\}_{j=1}^{M_i}$  be a set of independent solutions to the  $i^{th}$  task, observed at time  $t_i = \frac{i}{n}$ ,  $1 \leq i \leq n$ , with  $\theta_{ij} \in \mathbb{R}^p$  and  $\theta_{ij} \sim P(\cdot, t_i)$ . Notice that, at time  $t_i$ , we allow to tackle  $M_i$  times the task coming from the distribution  $P(\cdot, t_i)$ , for the sake of generality. Moreover, let  $M_i$  be a discrete random variable for each  $i$ . Finally, let us introduce a Time-Variant Kernel Density Estimator of this form:

$$\hat{p}(\theta, t) = \frac{1}{a_0(-\rho)N(t)\lambda|H|^{\frac{1}{2}}} \sum_{t_i=\frac{1}{n}}^t K_T\left(\frac{t-t_i}{\lambda}\right) \sum_{j=1}^{M_i} K_S(H^{-\frac{1}{2}}(\theta - \theta_{ij})) \quad (3)$$

which is based on [10] and will be used as a prior in order to model a time-variant distribution on the solved tasks. The factor  $a_0(-\rho) = \int_{-\rho}^1 K_T(t)dt$  is used to perform the boundary correction, recovering consistency at the boundaries [12], therefore also in  $t = 1$ .  $K_T$  is the temporal kernel, whereas  $K_S$  is the multivariate non-negative spatial kernel.

Now under the following assumptions (also stated in [10]):

**Assumption 3.1** (Task independence). *For  $1 \leq i \neq i' \leq n, 1 \leq j \leq M_i$ , and  $1 \leq j' \leq M_{i'}$ ,  $\theta_{ij}$  and  $\theta_{i'j'}$  are independent;*

**Assumption 3.2** (Differentiable density function).  *$p(\theta, t_i) : \mathbb{R}^p \times [0, 1] \rightarrow \mathbb{R}$  is twice differentiable for every  $t_i$ ,  $\theta_{ij}$ ;*

**Assumption 3.3** (Lipschitz continuity w.r.t. time).  *$|p(\theta, t_2) - p(\theta, t_1)| \leq L|t_2 - t_1|$ , for  $\theta \in \mathbb{R}^p$ ,  $L \in \mathbb{R}^+$ ;*

**Assumption 3.4** (On the spatial kernel). *Let  $\alpha = (\alpha_1, \dots, \alpha_p)$  be a multi-index, with  $\alpha_i \geq 0$  for  $i = 1, \dots, p$ ,  $\theta^\alpha = \prod_{i=1}^p \theta_i^{\alpha_i}$  for each  $\theta \in \mathbb{R}^p$ , and  $N_0$  is an index set where all  $p$  components of each member are either 0 or even integers.*

$$\begin{aligned} \int_{\mathbb{R}^p} K_S(\theta) d\theta = 1, \lim_{\|\theta\| \rightarrow \infty} \|\theta\|^p K_S(\theta) = 0, \int_{\mathbb{R}^p} \theta^\alpha K_S(\theta) d\theta = \mu_\alpha \leq \infty, \alpha \in N_0, \\ \int_{\mathbb{R}^p} \theta^\alpha K_S(\theta) d\theta = 0, \alpha \notin N_0; \end{aligned}$$

**Assumption 3.5** (On the temporal kernel).

$$\int_{-c}^c K_T(t) dt = 1, \int_{-c}^c t K_T(t) dt = 0, \int_{-c}^c t^2 K_T(t) dt = \sigma_T \leq \infty;$$

we can write

**Theorem 3.6** (Uniform consistency of the density estimator). *Assume 3.1 - 3.5. Moreover, assume that  $K_S$  is spherically symmetric, with a bounded, Hölder-continuous derivative, that  $K_T$  is a Hölder-continuous and compactly supported kernel on a subset of  $\mathbb{R}$ , that all the  $M_i$ s are independent and identically distributed random variables with mean  $m > 0$  and all moments finite, independent of the  $\theta_{ij}$ s, and that  $p(\theta, t)$ , viewed as a  $(p+1)$ -variate function on  $\mathbb{R}^p \times (0, 1]$ , has two bounded derivatives. Take  $H$  and  $\lambda$  such that  $|H|^{\frac{1}{2}}(n) \rightarrow 0$ ,  $\lambda(n) \rightarrow 0$  and  $n^{1-\epsilon}|H|^{\frac{1}{2}}\lambda \rightarrow \infty$  for some  $\epsilon > 0$  as  $n \rightarrow \infty$ , then*

$$\hat{p}(\theta, t) = p(\theta, t) + O[(N(t)|H|\lambda)^{-\frac{1}{2}}(\log n)^{\frac{1}{2}} + \text{tr}(H) + \lambda]$$

*uniformly in  $(\theta, t) \in \mathcal{K} \times \mathcal{I}$ , with probability 1, where  $\mathcal{K}$  is a compact subset of  $\mathbb{R}^p$  and  $\mathcal{I}$  is a compact subset of  $(0, 1]$ .*

A proof of the above theorem is shown in Appendix A and leverages the same approach as in [10] being a weaker version, in terms of convergence rate, of their Theorem 1. This weakening was necessary in order to obtain an upper bound in closed-form expression of the KL-Divergence between the prior and the posterior in Equation 2. Indeed, if we choose  $q_\xi(\theta) = \frac{1}{K} \sum_{k=1}^K \mathcal{N}(\theta | \mu_k, \Sigma_k)$ , with variational parameter  $\xi = (\mu_1, \dots, \mu_K, \Sigma_1, \dots, \Sigma_K)$ , and we choose  $K_S$  as a Gaussian kernel, then for a fixed time instant  $t$  our prior is a mixture of Gaussians with non-uniform weights. Therefore, through the upper bound on the KL-Divergence shown in Appendix B, we have that the ELBO upper bounds the KL-Divergence between the approximate and the exact posterior. Since the covariance matrices of the posterior must be positive definite, we will learn the factor  $L$  of their Cholesky decomposition as in [35].

## 4 Finite Sample Analysis

In order to provide a finite sample analysis of Algorithm 1 based on the prior of Section 3, we will extend Theorem 2 of [35] in our context, enabling also a theoretical comparison between the two respective versions of Algorithm 1. Therefore, considering the family of linearly parametrized value

functions,  $Q_\theta(s, a) = \theta^T \phi(s, a)$ , having bounded weights  $\|\theta\|_2 \leq \theta_{max}$  and uniformly bounded features  $\|\phi(s, a)\|_2 \leq \phi_{max}$ , and assuming only finite data are available, we can bound the expected mellow Bellman error under the variational distribution minimizing Equation (2) for any fixed target task  $\mathcal{M}_i$  through the following theorem.

**Theorem 4.1** (Bound on the expected mellow Bellman error). *Let  $\hat{\xi}$  be the variational parameter minimizing Equation (2) on a dataset  $D$  of  $N$  i.i.d. samples distributed according to  $\mathcal{M}_i$  and  $\nu$ . Moreover, let  $\theta^* = \arg \inf_\theta \|\tilde{B}_\theta\|_\nu^2$  and define  $v(\theta^*) = \mathbb{E}_{\mathcal{N}(\theta^*, \frac{1}{N}I)}[v(\theta)]$ , with  $v(\theta) = \mathbb{E}_\nu[\text{Var}_{\mathcal{P}_i}[\tilde{b}(\theta)]]$ , where  $\tilde{b}(\theta) = r + \gamma \text{mellow-max}_{a'} Q_\theta(s', a') - Q_\theta(s, a)$ . Then, there exist constants  $c_1, c_2, c_3$  such that with probability at least  $1 - \delta$  over the choice of  $D$ :*

$$\mathbb{E}_{q_\xi} \left[ \left\| \tilde{B}_\theta \right\|_\nu^2 \right] \leq 2 \left\| \tilde{B}_{\theta^*} \right\|_\nu^2 + v(\theta^*) + c_1 \sqrt{\frac{\log \frac{2}{\delta}}{N}} + \frac{c_2 + \psi p \log N + \psi \varphi(\Theta_s)}{N} + \frac{c_3}{N^2},$$

where

$$\varphi(\Theta_s) = \frac{1}{\sigma^2} \sum_{j: \theta_j \in \Theta_s} \frac{c_j^{\hat{p}} e^{-\beta \|\theta^* - \theta_j\|}}{\sum_{j': \theta_{j'} \in \Theta_s} c_{j'}^{\hat{p}} e^{-\beta \|\theta^* - \theta_{j'}\|}} \|\theta^* - \theta_j\|, \quad (4)$$

assuming the matrix  $H$  of Equation (3) to be an isotropic covariance matrix with variance  $\sigma^2$ ,  $\beta = \frac{1}{2\sigma^2}$  and  $c_j^{\hat{p}}$  the weight assigned to the  $j^{\text{th}}$  prior component. Furthermore, we are assuming  $M_i = 1$  for each  $i$  in our estimator.

The above theorem shows the difference between the plain mixture version of Algorithm 1 [35] and our solution. Indeed, looking at  $\varphi(\Theta_s)$ , we are able to shed some light on the different theoretical properties of the two versions. More specifically, in the plain mixture version, the factor  $c_j^{\hat{p}}$  does not appear, which implies a uniform importance of the source solutions  $\Theta_s$  w.r.t. the target task. On the other hand, in our version of the algorithm, we are able to give different importance to each source solution through  $c_j^{\hat{p}}$ . In our time-variant scenario, this importance will be higher on the more recent solutions w.r.t. the older ones, potentially allowing a reduction of the term  $\varphi(\Theta_s)$  in contrast to the time-invariant version. A proof for the above theorem is given in Appendix C.

## 5 Related Works

Our work is built upon [35], but differs from it because we leverage a time-variant structure underlying the task generating process, which is not taken into account in [35]. A theoretical comparison between the two solutions is available in Section 4 through Theorem 4.1, whereas the experimental comparison is in Section 6. Furthermore, our work relates to both [38], which deals with finite MDPs, and [17], which leverages commonalities in the value function structure, but, in contrast to our work, they do not account for a time-variant distribution. The work done in [6, 13, 26] leverage latent embeddings in order to model variations between the tasks, which eventually are solved through a model-based RL algorithm, on the other hand, we use a model-free approach.

Another related work has been done in [9] where they develop a low theoretical regret algorithm accounting for potential underlying dynamics. However, they use the online learning framework, whereas we are working in a transfer learning setting. Moreover, in [7], they learn a prior from videos (mainly to model the physical dynamics) and incorporate it into a model-based RL algorithm, whereas in [39] a single episode policy transfer methodology has been developed leveraging variational inference, but for contexts where the differences in dynamics can be identified in the early steps of an episode. Finally, in the context of supervised learning, our work relates also to [23], which proposes a transfer learning mechanism in the context of a possibly non-stationary environment through a weighting approach, and [22], which, instead, does transfer in non-stationary environments through ensembles.

## 6 Experiments

In this section, we compare our time-variant solution for transfer learning with the associated non-time-variant solution of [35] in three different domains with three different time dynamics. A detailed description of the used parameters together with the analytical expression of the employed dynamics are provided in Appendix D.

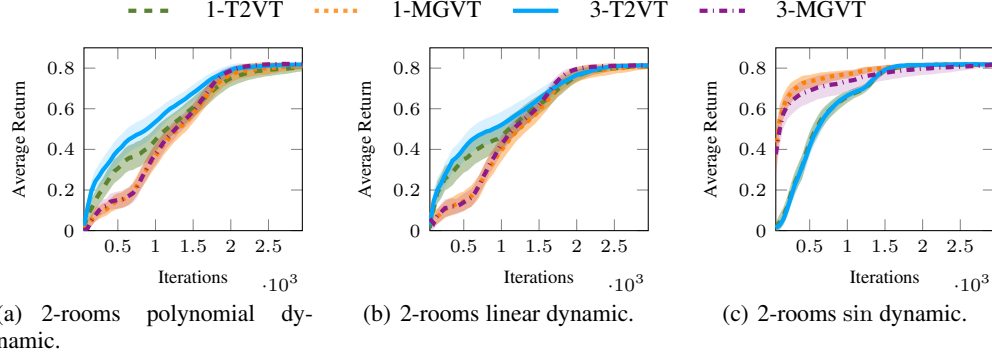


Figure 1: Average return achieved by the algorithms with 95% confidence intervals computed using 50 independent runs.

## 6.1 Time-Dynamics

The distribution over the tasks is usually a given distribution over one or more parameters defining the task itself. Therefore, in order to obtain time-variance in such distribution, we will vary its mean through time according to a certain dynamic. These dynamics are linear, polynomial, and sinusoidal. In the context of these experiments, we will use a time-variant Gaussian distribution, clipping its realizations within the domain of the parameters defining the task (for further details see Appendix D).

## 6.2 Two-Rooms Environment

In this setting, we have an agent navigating two rooms separated by a wall. The agent starts from the bottom-left corner and must reach the opposite one. The only way to reach this goal is to pass through the door whose position is unknown to the agent. The actions available to the agent are *up*, *down*, *left*, and *right*, which allow the agent to move in the respective directions by one position, unless he/she hits a wall (in this last case the position remains unchanged). Furthermore, the final position of the agent after a movement action is altered by Gaussian noise  $\mathcal{N}(0, 0.2)$ . The state space is modeled through a  $10 \times 10$  continuous grid. Finally, the reward function is 0 everywhere except in the goal state, where is 1. The discount factor  $\gamma = 0.99$ . For this setting, we used linearly parametrized  $Q$ -functions with 121 equally-spaced radial basis features.

We considered ten time instants available in the source tasks to learn the target, corresponding to the eleventh time instant. Therefore, we sampled five tasks from the time-variant distribution for each  $i = 1, \dots, 11$ . The parameter defining the task is the door location, hence the time-variant distribution is over that parameter, as we already mentioned in Section 6.1. We solve all the source tasks by directly minimizing the TD error, then we exploit the learned solutions to perform transfer over the target. We compare our time-variant variational transfer algorithm leveraging a  $c$ -components posterior ( $c$ -T2VT) with the mixture of Gaussian variational transfer using still  $c$ -components ( $c$ -MGVT)[35]. More specifically, our time-variant prior will consider the source task solutions as equally spaced samples in the time interval  $[0, 1]$ , moreover, in order to perform transfer to the eleventh task, we will use the distribution given by our estimator for  $t = 1$ . Finally, the temporal kernel will be Epanechnikov in the context of all the experiments.

The average return over the last 50 learning episodes as a function of the number of training iterations is shown in Figure 1, for the time dynamics mentioned in Section 6.1. Each learning curve is computed using 50 independent runs, each one resampling both the source and target tasks, with 95% confidence intervals. For the polynomial and linear dynamics, we can see an advantage of our technique in the early learning iterations. The sinusoidal dynamic is designed to disadvantage our technique w.r.t.  $c$ -MGVT, indeed, it makes the target task appear twice in the sources. This fact inevitably favors  $c$ -MGVT, which will give a higher weight to those source tasks being sampled from the same distribution of the target. Observe that  $c$ -MGVT gives uniform weights to all the source tasks, hence increasing the replicas importance within the sources, whereas  $c$ -T2VT gives increasing weights the more recent the source solution.

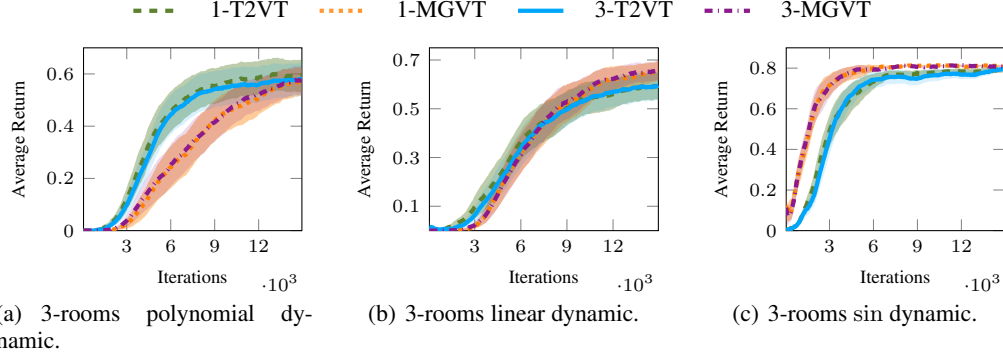


Figure 2: Average return achieved by the algorithms with 95% confidence intervals computed using 50 independent runs.

### 6.3 Three-Rooms Environment

This scenario is an extension of the previous one, hence the environmental settings remain the same, the agent has just an additional wall to traverse in order to reach his/her goal. Of course, the position of the door for this additional wall is still unknown to the agent. In order to increase the complexity of the dynamics, we let the two doors move in opposite directions starting at the two far ends of the room, each door with the same dynamic. In Figure 2, we compare  $c$ -T2VT with  $c$ -MGVT using still 95% confidence intervals. For what concern the polynomial dynamic, we observe a better performance of  $c$ -T2VT w.r.t.  $c$ -MGVT, whereas for the sinusoidal dynamic, we have essentially the same behavior as in the two rooms environment. Finally, in the linear dynamic, we observe that the performance difference of the two algorithms is not statistically significant.

### 6.4 Mountain Car

In this section, we consider a classic control environment known as Mountain Car [30]. In Mountain Car the agent is an underpowered car whose goal consists in escaping a valley. Due to the limitation to its engine, the car has to alternately drive up along the two slopes of the valley in order to gain sufficient momentum to overcome gravity. In Figure 3, we have a comparison between  $c$ -T2VT and  $c$ -MGVT on the three proposed dynamics. We observe a statistically significant improvement in the polynomial dynamic across the whole learning process for  $c$ -T2VT, which extends also to the sinusoidal dynamic case. We would like to highlight the differences between the sinusoidal dynamic in Mountain Car w.r.t. the previous two environments. Here our algorithm is able to perform better due to a bias-variance trade-off in its favor. More specifically, the value functions vary more rapidly in Mountain Car than in the rooms environment in face of a change in the task-defining parameters. Therefore, our prior estimator has less variance, since it considers only the latest sources, at the cost of a bias increase, because it discards the first task which has the same parametrization as the target (due to the periodicity of the sin function).  $c$ -MGVT considers all the source tasks with the same uniform weight, hence it is able to consider the tasks which have an equivalent parametrization to the target, but are farther behind in the history of the sources. This fact decreases the bias at the cost of accepting more variance in the prior estimation. In Mountain Car the trade-off proposed by our algorithm is more advantageous w.r.t. that one proposed by  $c$ -MGVT due to the more rapidly changing behavior of the value functions. For what concerns the linear dynamic, we do not observe a statistically significant difference in performance between the two algorithms.

## 7 Discussion and Conclusions

In this paper, we presented a time-variant approach for transferring value functions through a variational scheme. In order to deal with a time-variant distribution of the tasks, we have devised a suitable estimator for the prior to be used in the variational scheme providing its uniform consistency over a compact subset of  $\mathbb{R}^p \times (0, 1]$ . We have, then, provided a finite sample analysis on the performance of the variational transfer algorithm based on our estimator, enabling a theoretical

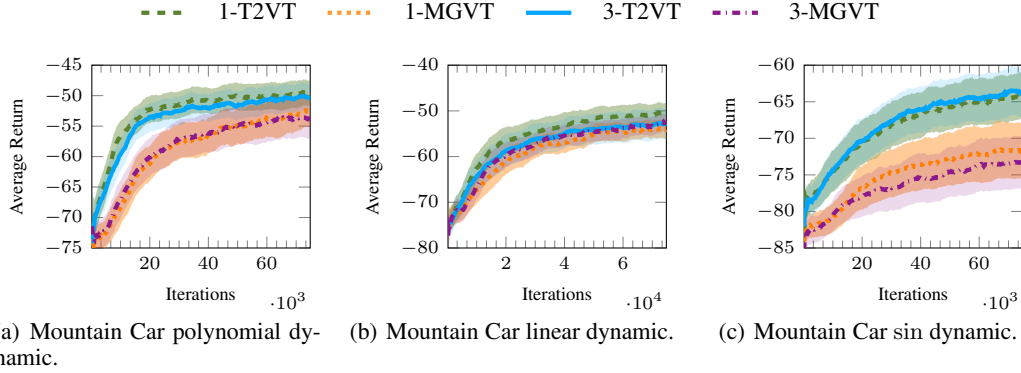


Figure 3: Average return achieved by the algorithms with 95% confidence intervals computed using 50 independent runs.

comparison with the time-invariant version of [35]. Finally, we have experimentally proved our algorithm abilities to deal with time-variant distributions.

Notice that discriminating the source tasks according to time is an additional step bringing transfer learning approaches and learning in non-stationary environments a bit closer together [21]. It is also important to highlight the fact that, instead of considering time, we could switch to any other variable (e.g., the parameter defining the task itself) as long as it is available together with each source solution and we can properly remap it into  $(0, 1]$ . This could allow us to leverage completely different structures in order to perform transfer to the target task. Moreover, to further improve the capabilities of the algorithm to deal with time-variant distributions would be relevant to leverage Gaussian Processes with a non-stationary covariance function as a future work [28]. Finally, we would like also to highlight the possibility to use this time-variant transfer paradigm also in lifelong learning scenarios [5] as a potential future direction.

## Broader Impact

Authors are required to include a statement of the broader impact of their work, including its ethical aspects and future societal consequences. Authors should discuss both positive and negative outcomes, if any. For instance, authors should discuss a) who may benefit from this research, b) who may be put at disadvantage from this research, c) what are the consequences of failure of the system, and d) whether the task/method leverages biases in the data. If authors believe this is not applicable to them, authors can simply state this.

Use unnumbered first level headings for this section, which should go at the end of the paper. **Note that this section does not count towards the eight pages of content that are allowed.**

## Acknowledgments and Disclosure of Funding

Use unnumbered first level headings for the acknowledgments. All acknowledgments go at the end of the paper before the list of references. Moreover, you are required to declare funding (financial activities supporting the submitted work) and competing interests (related financial activities outside the submitted work). More information about this disclosure can be found at: <https://neurips.cc/Conferences/2020/PaperInformation/FundingDisclosure>.

Do **not** include this section in the anonymized submission, only in the final paper. You can use the ack environment provided in the style file to automatically hide this section in the anonymized submission.



## References

- [1] Maruan Al-Shedivat, Trapit Bansal, Yuri Burda, Ilya Sutskever, Igor Mordatch, and Pieter Abbeel. Continuous adaptation via meta-learning in nonstationary and competitive environments. *arXiv preprint arXiv:1710.03641*, 2017.
- [2] André Barreto, Will Dabney, Rémi Munos, Jonathan J Hunt, Tom Schaul, Hado P van Hasselt, and David Silver. Successor features for transfer in reinforcement learning. In *Advances in neural information processing systems*, pages 4055–4065, 2017.
- [3] David M Blei, Alp Kucukelbir, and Jon D McAuliffe. Variational inference: A review for statisticians. *Journal of the American statistical Association*, 112(518):859–877, 2017.
- [4] Olivier Catoni. Pac-bayesian supervised classification: the thermodynamics of statistical learning. *arXiv preprint arXiv:0712.0248*, 2007.
- [5] Zhiyuan Chen and Bing Liu. Lifelong machine learning. *Synthesis Lectures on Artificial Intelligence and Machine Learning*, 12(3):1–207, 2018.
- [6] Finale Doshi-Velez and George Konidaris. Hidden parameter markov decision processes: A semiparametric regression approach for discovering latent task parametrizations. In *IJCAI: proceedings of the conference*, volume 2016, page 1432. NIH Public Access, 2016.
- [7] Yilun Du and Karthic Narasimhan. Task-agnostic dynamics priors for deep reinforcement learning. In *International Conference on Machine Learning*, pages 1696–1705, 2019.
- [8] Fernando Fernández and Manuela Veloso. Probabilistic policy reuse in a reinforcement learning agent. In *Proceedings of the fifth international joint conference on Autonomous agents and multiagent systems*, pages 720–727, 2006.
- [9] Eric C Hall and Rebecca M Willett. Online convex optimization in dynamic environments. *IEEE Journal of Selected Topics in Signal Processing*, 9(4):647–662, 2015.
- [10] Peter Hall, Hans-Georg Müller, and Ping-Shi Wu. Real-time density and mode estimation with application to time-dynamic mode tracking. *Journal of Computational and Graphical Statistics*, 15(1):82–100, 2006.
- [11] John R Hershey and Peder A Olsen. Approximating the kullback leibler divergence between gaussian mixture models. In *2007 IEEE International Conference on Acoustics, Speech and Signal Processing-ICASSP'07*, volume 4, pages IV–317. IEEE, 2007.
- [12] M Chris Jones. Simple boundary correction for kernel density estimation. *Statistics and computing*, 3(3):135–146, 1993.
- [13] Taylor W Killian, Samuel Daulton, George Konidaris, and Finale Doshi-Velez. Robust and efficient transfer learning with hidden parameter markov decision processes. In *Advances in neural information processing systems*, pages 6250–6261, 2017.
- [14] Diederik P Kingma and Jimmy Ba. Adam: A method for stochastic optimization. *arXiv preprint arXiv:1412.6980*, 2014.
- [15] George Konidaris and Andrew G Barto. Building portable options: Skill transfer in reinforcement learning. In *IJCAI*, volume 7, pages 895–900, 2007.
- [16] Alessandro Lazaric. Transfer in reinforcement learning: a framework and a survey. In *Reinforcement Learning*, pages 143–173. Springer, 2012.
- [17] Alessandro Lazaric and Mohammad Ghavamzadeh. Bayesian multi-task reinforcement learning. In *Proceedings of the 27th International Conference on International Conference on Machine Learning*, pages 599–606, 2010.
- [18] Alessandro Lazaric, Marcello Restelli, and Andrea Bonarini. Transfer of samples in batch reinforcement learning. In *Proceedings of the 25th international conference on Machine learning*, pages 544–551, 2008.
- [19] Lucas Lehnert and Michael L Littman. Transfer with model features in reinforcement learning. *arXiv preprint arXiv:1807.01736*, 2018.
- [20] Odalric-Ambrym Maillard, Rémi Munos, Alessandro Lazaric, and Mohammad Ghavamzadeh. Finite-sample analysis of bellman residual minimization. In *Proceedings of 2nd Asian Conference on Machine Learning*, pages 299–314, 2010.

- [21] Leandro L Minku. Transfer learning in non-stationary environments. In *Learning from Data Streams in Evolving Environments*, pages 13–37. Springer, 2019.
- [22] Leandro L Minku and Xin Yao. Ddd: A new ensemble approach for dealing with concept drift. *IEEE transactions on knowledge and data engineering*, 24(4):619–633, 2011.
- [23] Leandro L Minku and Xin Yao. How to make best use of cross-company data in software effort estimation? In *Proceedings of the 36th International Conference on Software Engineering*, pages 446–456, 2014.
- [24] Anusha Nagabandi, Ignasi Clavera, Simin Liu, Ronald S Fearing, Pieter Abbeel, Sergey Levine, and Chelsea Finn. Learning to adapt in dynamic, real-world environments through meta-reinforcement learning. *arXiv preprint arXiv:1803.11347*, 2018.
- [25] OpenAI, Christopher Berner, Greg Brockman, Brooke Chan, Vicki Cheung, Przemysław Dębiak, Christy Dennison, David Farhi, Quirin Fischer, Shariq Hashme, Chris Hesse, Rafal Józefowicz, Scott Gray, Catherine Olsson, Jakub Pachocki, Michael Petrov, Henrique Pondé de Oliveira Pinto, Jonathan Raiman, Tim Salimans, Jeremy Schlatter, Jonas Schneider, Szymon Sidor, Ilya Sutskever, Jie Tang, Filip Wolski, and Susan Zhang. Dota 2 with large scale deep reinforcement learning. 2019.
- [26] Christian F Perez, Felipe Petroski Such, and Theofanis Karaletsos. Generalized hidden parameter mdps transferable model-based rl in a handful of trials. *arXiv preprint arXiv:2002.03072*, 2020.
- [27] Martin L Puterman. *Markov decision processes: discrete stochastic dynamic programming*. John Wiley & Sons, 2014.
- [28] Sami Remes, Markus Heinonen, and Samuel Kaski. Non-stationary spectral kernels. In *Advances in Neural Information Processing Systems*, pages 4642–4651, 2017.
- [29] David Silver, Thomas Hubert, Julian Schrittwieser, Ioannis Antonoglou, Matthew Lai, Arthur Guez, Marc Lanctot, Laurent Sifre, Dhharshan Kumaran, Thore Graepel, et al. A general reinforcement learning algorithm that masters chess, shogi, and go through self-play. *Science*, 362(6419):1140–1144, 2018.
- [30] Richard S Sutton and Andrew G Barto. Reinforcement learning: An introduction. 2011.
- [31] Matthew E Taylor, Nicholas K Jong, and Peter Stone. Transferring instances for model-based reinforcement learning. In *Joint European conference on machine learning and knowledge discovery in databases*, pages 488–505. Springer, 2008.
- [32] Matthew E. Taylor and Peter Stone. Transfer learning for reinforcement learning domains: A survey. *Journal of Machine Learning Research*, 10(56):1633–1685, 2009.
- [33] Matthew E Taylor, Peter Stone, and Yaxin Liu. Transfer learning via inter-task mappings for temporal difference learning. *Journal of Machine Learning Research*, 8(Sep):2125–2167, 2007.
- [34] Andrea Tirinzoni, Mattia Salvini, and Marcello Restelli. Transfer of samples in policy search via multiple importance sampling. In *International Conference on Machine Learning*, pages 6264–6274, 2019.
- [35] Andrea Tirinzoni, Rafael Rodriguez Sanchez, and Marcello Restelli. Transfer of value functions via variational methods. In *Advances in Neural Information Processing Systems*, pages 6179–6189, 2018.
- [36] Andrea Tirinzoni, Andrea Sessa, Matteo Pirotta, and Marcello Restelli. Importance weighted transfer of samples in reinforcement learning. *arXiv preprint arXiv:1805.10886*, 2018.
- [37] Oriol Vinyals, Igor Babuschkin, Wojciech M Czarnecki, Michaël Mathieu, Andrew Dudzik, Junyoung Chung, David H Choi, Richard Powell, Timo Ewalds, Petko Georgiev, et al. Grandmaster level in starcraft ii using multi-agent reinforcement learning. *Nature*, 575(7782):350–354, 2019.
- [38] Aaron Wilson, Alan Fern, Soumya Ray, and Prasad Tadepalli. Multi-task reinforcement learning: a hierarchical bayesian approach. In *Proceedings of the 24th international conference on Machine learning*, pages 1015–1022, 2007.
- [39] Jiachen Yang, Brenden Petersen, Hongyuan Zha, and Daniel Faissol. Single episode policy transfer in reinforcement learning. In *International Conference on Learning Representations*, 2020.

## A Proof of Theorem 3.6

**Definition A.1.** For a spatial kernel  $K_S$ :  $\mu_l(K_S) = \int y^l K_S(\theta) d\theta$

**Definition A.2.** For a temporal kernel  $K_T$ :  $a_l(-\rho) = \int_{-\rho}^1 t^l K_T(t) dt$

**Lemma A.1** (Estimator consistency on the right boundary). *Let  $t \in B_r = \{\tau : 1 - \lambda \leq \tau \leq 1\}$  then under assumptions of Theorem 3.6:*

$$\mathbb{E}[\hat{p}(\theta, t) | \mathcal{M}] = p(\theta, t) + O(\lambda) + O(tr(H)),$$

where  $\mathcal{M}$  represents all the discrete random variables  $M_i$  for  $i = 1 \dots n$ .

*Proof.*

$$\begin{aligned} \mathbb{E}[\hat{p}(\theta, t) | \mathcal{M}] &= \\ &= \frac{1}{N(t)\lambda|H|^{\frac{1}{2}}a_0(-\rho)} \sum_{t_i=\frac{1}{n}}^t \int K_T\left(\frac{t-\tau}{\lambda}\right) \sum_{j=1}^{M_i} \int_{-\infty}^{+\infty} K_S\left(H^{-\frac{1}{2}}(\theta-x)\right) p(x, \tau) dx d\tau \end{aligned} \quad (5)$$

$$= \frac{1}{N(t)\lambda|H|^{\frac{1}{2}}a_0(-\rho)} \sum_{t_i=\frac{1}{n}}^t \int K_T\left(\frac{t-\tau}{\lambda}\right) \sum_{j=1}^{M_i} \int_{+\infty}^{-\infty} -K_S(y)p(\theta - H^{\frac{1}{2}}y, \tau) |H|^{\frac{1}{2}} dy d\tau \quad (6)$$

$$\begin{aligned} &= \frac{1}{N(t)\lambda a_0(-\rho)} \sum_{t_i=\frac{1}{n}}^t \int K_T\left(\frac{t-\tau}{\lambda}\right) \sum_{j=1}^{M_i} \int_{-\infty}^{+\infty} K_S(y) \left( p(\theta, \tau) - (H^{\frac{1}{2}}y)^T \nabla^S p(\theta, \tau) + \right. \\ &\quad \left. \frac{1}{2} (H^{\frac{1}{2}}y)^T \mathcal{H}^S p(\theta, \tau) (H^{\frac{1}{2}}y) + o(tr(H)) \right) dy d\tau \end{aligned} \quad (7)$$

$$\begin{aligned} &= \frac{1}{N(t)\lambda a_0(-\rho)} \sum_{t_i=\frac{1}{n}}^t \int K_T\left(\frac{t-\tau}{\lambda}\right) M_i \left( \int_{-\infty}^{+\infty} K_S(y) p(\theta, \tau) dy \right. \\ &\quad \left. - \int_{-\infty}^{+\infty} K_S(y) (H^{\frac{1}{2}}y)^T \nabla^S p(\theta, \tau) dy + \right. \\ &\quad \left. \int_{-\infty}^{+\infty} \frac{1}{2} K_S(y) (H^{\frac{1}{2}}y)^T \mathcal{H}^S p(\theta, \tau) (H^{\frac{1}{2}}y) dy + o(tr(H)) \right) d\tau \end{aligned} \quad (8)$$

$$\begin{aligned} &= \frac{1}{N(t)\lambda a_0(-\rho)} \sum_{t_i=\frac{1}{n}}^t \int K_T\left(\frac{t-\tau}{\lambda}\right) M_i \left( p(\theta, \tau) + \right. \\ &\quad \left. \frac{1}{2} \mu_2(K_S) tr(H \mathcal{H}^S p(\theta, \tau)) + o(tr(H)) \right) d\tau \end{aligned} \quad (9)$$

$$= \frac{1}{\lambda a_0(-\rho)} \int_{\frac{t-1}{\lambda}}^{\frac{t}{\lambda}} K_T\left(\frac{t-\tau}{\lambda}\right) \left( p(\theta, \tau) + O(tr(H)) \right) d\tau \quad (10)$$

$$= \frac{1}{\lambda a_0(-\rho)} \left( \int_{-\rho}^1 K_T\left(\frac{t-\tau}{\lambda}\right) p(\theta, \tau) d\tau + O(tr(H)) \int_{-\rho}^1 K_T\left(\frac{t-\tau}{\lambda}\right) d\tau \right) \quad (11)$$

$$= \frac{\lambda}{\lambda a_0(-\rho)} \left( - \int_1^{-\rho} K_T(v) p(\theta, t - \lambda v) dv - O(tr(H)) \int_1^{-\rho} K_T(v) dv \right) \quad (12)$$

$$\begin{aligned} &= \frac{1}{a_0(-\rho)} \left( \int_{-\rho}^1 K_T(v) \left( p(\theta, t) - \lambda v p'(\theta, t) + \right. \right. \\ &\quad \left. \left. \frac{1}{2} \lambda^2 v^2 p''(\theta, t) + o(\lambda^2) \right) dv + O(tr(H)) \right) \end{aligned} \quad (13)$$

$$= p(\theta, t) - \lambda p'(\theta, t) \frac{a_1(-\rho)}{a_0(-\rho)} + O(\lambda^2) + O(tr(H)) \quad (14)$$

$$= p(\theta, t) + O(\lambda) + O(tr(H)), \quad (15)$$

where in (6) we performed a change of variable,  $y = H^{-\frac{1}{2}}(\theta - x)$ , in (7) we used the following Taylor expansion:

$$p(\theta - H^{\frac{1}{2}}y, \tau) = p(\theta, \tau) - (H^{\frac{1}{2}}y)^T \nabla^S p(\theta, \tau) + \frac{1}{2}(H^{\frac{1}{2}}y)^T \mathcal{H}^S p(\theta, \tau)(H^{\frac{1}{2}}y) + o(\text{tr}(H)),$$

in (8) we used Assumption 3.4, in (9) we used Definition A.1, in (10) we used  $\frac{t-\tau}{\lambda} \in [\frac{t-1}{\lambda}, \frac{t}{\lambda})$ , in 11 we set  $t = 1 - \rho\lambda$ , which implies  $\frac{t-\tau}{\lambda} \in [-\rho, \frac{1}{\lambda} - \rho)$ , then we used the support of  $K_T$  (assumed to be  $[-1, 1]$  without loss of generality) since  $\lambda \rightarrow 0$ . Finally, in 12 we used a change of variable,  $\frac{t-\tau}{\lambda} = v$ , and in 13 we used the following Taylor expansion:

$$p(\theta, t - \lambda v) = p(\theta, t) - \lambda v p'(\theta, t) + \frac{1}{2} \lambda^2 v^2 p''(\theta, v) + o(\lambda^2).$$

□

Notice that we reported the consistency proof only on the right boundary because is the one we use in the context of our algorithm. The above procedure can be easily adjusted to prove consistency of the estimator on the left boundary getting the same convergence rate. Moreover, analogously, we can obtain consistency away from the two boundaries with a convergence rate squared w.r.t.  $\lambda$ .

**Definition A.3.** For a spatial kernel  $K_S$ :  $R(K_S) = \int K_S^2(\theta) d\theta$

**Definition A.4.** For a temporal kernel  $K_T$ :  $b_{K_T}(-\rho) = \int_{-\rho}^1 K_T^2(t) dt$

**Lemma A.2** (Variance of the estimator on the right boundary). *Let  $t \in B_r = \{\tau : 1 - \lambda \leq \tau \leq 1\}$  then under assumptions of Theorem 3.6:*

$$\mathbb{V}ar[\hat{p}(\theta, t) | \mathcal{M}] \leq \frac{C_1}{N(t) |H|^{\frac{1}{2}} \lambda},$$

where  $\mathcal{M}$  represents all the discrete random variables  $M_i$  for  $i = 1 \dots n$ .

*Proof.*

$$\mathbb{V}ar[\hat{p}(\theta, t)|\mathcal{M}] = \frac{1}{N(t)a_0^2(-\rho)} \mathbb{V}ar \left[ \frac{1}{|H|^{\frac{1}{2}}\lambda} K_T \left( \frac{t-t_i}{\lambda} \right) K_S \left( H^{-\frac{1}{2}}(\theta - x_{ij}) \right) \right] \quad (16)$$

$$= \frac{1}{N(t)a_0^2(-\rho)} \left( \mathbb{E} \left[ \frac{1}{|H|^{\frac{1}{2}}\lambda^2} K_T^2 \left( \frac{t-t_i}{\lambda} \right) K_S^2 \left( H^{-\frac{1}{2}}(\theta - x_{ij}) \right) \right] - \mathbb{E}^2 \left[ \frac{1}{|H|^{\frac{1}{2}}\lambda} K_T \left( \frac{t-t_i}{\lambda} \right) K_S \left( H^{-\frac{1}{2}}(\theta - x_{ij}) \right) \right] \right) \quad (17)$$

$$= \frac{1}{N(t)a_0^2(-\rho)} \left( \int \frac{1}{|H|^{\frac{1}{2}}\lambda^2} K_T^2 \left( \frac{t-\tau}{\lambda} \right) \int_{+\infty}^{-\infty} -|H|^{\frac{1}{2}} K_S^2(y) p(\theta - H^{\frac{1}{2}}y, \tau) dy d\tau - \left( \int \frac{1}{|H|^{\frac{1}{2}}\lambda} K_T \left( \frac{t-\tau}{\lambda} \right) \int_{+\infty}^{-\infty} -|H|^{\frac{1}{2}} K_S(y) p(\theta - H^{\frac{1}{2}}y, \tau) dy d\tau \right)^2 \right) \quad (18)$$

$$= \frac{1}{N(t)a_0^2(-\rho)} \left( \int \frac{1}{|H|^{\frac{1}{2}}\lambda^2} K_T^2 \left( \frac{t-\tau}{\lambda} \right) \int_{-\infty}^{+\infty} K_S^2(y) (p(\theta, \tau) + o(1)) dy d\tau - \left( \int \frac{1}{\lambda} K_T \left( \frac{t-\tau}{\lambda} \right) \int_{-\infty}^{+\infty} K_S(y) (p(\theta, \tau) + o(1)) dy d\tau \right)^2 \right) \quad (19)$$

$$= \frac{1}{N(t)a_0^2(-\rho)} \left( \int \frac{1}{|H|^{\frac{1}{2}}\lambda^2} K_T^2 \left( \frac{t-\tau}{\lambda} \right) (p(\theta, \tau) + o(1)) R(K_S) d\tau - \left( \int \frac{1}{\lambda} K_T \left( \frac{t-\tau}{\lambda} \right) (p(\theta, \tau) + o(1)) d\tau \right)^2 \right) \quad (20)$$

$$= \frac{1}{N(t)a_0^2(-\rho)} \left( \int_{-\rho}^1 \frac{1}{|H|^{\frac{1}{2}}\lambda^2} K_T^2 \left( \frac{t-\tau}{\lambda} \right) (p(\theta, \tau) + o(1)) R(K_S) d\tau - \left( \int_{-\rho}^1 \frac{1}{\lambda} K_T \left( \frac{t-\tau}{\lambda} \right) (p(\theta, \tau) + o(1)) d\tau \right)^2 \right) \quad (21)$$

$$= \frac{1}{N(t)a_0^2(-\rho)} \left( \int_1^{-\rho} -\frac{1}{|H|^{\frac{1}{2}}\lambda} K_T^2(v) (p(\theta, t - \lambda v) + o(1)) R(K_S) dv - \left( \int_1^{-\rho} -K_T(v) (p(\theta, t - \lambda v) + o(1)) dv \right)^2 \right) \quad (22)$$

$$= \frac{1}{N(t)a_0^2(-\rho)} \left( \int_{-\rho}^1 \frac{1}{|H|^{\frac{1}{2}}\lambda} K_T^2(v) (p(\theta, t) + o(1)) R(K_S) dv - \left( \int_{-\rho}^1 K_T(v) (p(\theta, t) + o(1)) dv \right)^2 \right) \quad (23)$$

$$= \frac{1}{N(t)a_0^2(-\rho)} \left( \frac{p(\theta, t) + o(1)}{|H|^{\frac{1}{2}}\lambda} R(K_S) b_{K_T}(-\rho) - (a_0(-\rho)(p(\theta, t) + o(1)))^2 \right) \quad (24)$$

$$= \frac{p(\theta, t) R(K_S) b_{K_T}(-\rho)}{N(t)|H|^{\frac{1}{2}}\lambda a_0^2(-\rho)} + O \left( \frac{1}{N(t)|H|^{\frac{1}{2}}\lambda} \right) \quad (25)$$

$$= O \left( \frac{1}{N(t)|H|^{\frac{1}{2}}\lambda} \right) \rightarrow \exists C_1 : \mathbb{V}ar[\hat{p}(\theta, t)|\mathcal{M}] \leq \frac{C_1}{N(t)|H|^{\frac{1}{2}}\lambda}, \quad (26)$$

where in (18) we performed a change of variable,  $y = H^{-\frac{1}{2}}(\theta - x)$ , in (19) we used the following Taylor expansion:

$$p(\theta - H^{\frac{1}{2}}y, \tau) = p(\theta, \tau) + o(1),$$

in 20 we used Definition A.3, in 21 we considered the fact that  $t \in B_r$  as we have done in 10 and 11 of the proof of A.1, in 22 we performed a change of variable,  $\frac{t-\tau}{\lambda} = v$ , in 23 we used the following Taylor expansion:

$$p(\theta, t - \lambda v) = p(\theta, t) + o(1),$$

whereas in 24 we have used Definition A.4. Finally, in 26 we have used the fact that  $p(\theta, t)$  has bounded derivatives and is a pdf, therefore it has finite supremum.  $\square$

**Lemma A.3** (Bound on the absolute values). *Let  $t \in B_r = \{\tau : 1 - \lambda \leq \tau \leq 1\}$  then under assumptions of Theorem 3.6:*

$$|\hat{p}(\theta, t) - \mathbb{E}[\hat{p}(\theta, t)|\mathcal{M}]| \leq \frac{C_2}{N(t)|H|^{\frac{1}{2}}\lambda},$$

where  $\mathcal{M}$  represents all the discrete random variables  $M_i$  for  $i = 1 \dots n$ .

*Proof.*

$$|\hat{p}(\theta, t) - \mathbb{E}[\hat{p}(\theta, t)|\mathcal{M}]| = \left| \frac{1}{N(t)\lambda|H|^{\frac{1}{2}}a_0(-\rho)} K_T\left(\frac{t-t_i}{\lambda}\right) K_S(H^{-\frac{1}{2}}(\theta - x_{ij})) - \frac{p(\theta, t) + O(\lambda) + O(\text{tr}(H))}{N(t)} \right| \quad (27)$$

$$\leq \left| \frac{M_T M_S}{N(t)\lambda|H|^{\frac{1}{2}}a_0(-\rho)} - \frac{p(\theta, t) + O(\lambda) + O(\text{tr}(H))}{N(t)} \right| \quad (28)$$

$$= O\left(\frac{1}{N(t)\lambda|H|^{\frac{1}{2}}a_0(-\rho)}\right) \rightarrow \exists C_2 : |\hat{p}(\theta, t) - \mathbb{E}[\hat{p}(\theta, t)|\mathcal{M}]| \leq \frac{C_2}{N(t)|H|^{\frac{1}{2}}\lambda}, \quad (29)$$

where in 27 we used lemma A.1 and in 28 we used the fact that  $K_T$  has a compact support on  $\mathbb{R}$  and  $K_S$  has a supremum.  $\square$

Now the proof of Theorem 3.6 can follow.

*Proof.* Let  $\xi = C \left( \frac{\log n}{N(t)|H|^{\frac{1}{2}}\lambda} \right)^{\frac{1}{2}}$  and  $C_3 = \frac{1}{2 \max(C_1, \frac{C_2}{3})}$ , using Bernstein's inequality we can write:

$$\mathbb{P}(|\hat{p}(\theta, t) - \mathbb{E}[\hat{p}(\theta, t)|\mathcal{M}]| > \xi|\mathcal{M}) \leq 2 \exp \left( - \frac{\frac{1}{2}\xi^2}{\frac{C_1}{N(t)|H|^{\frac{1}{2}}\lambda} + \frac{1}{3} \frac{C_2\xi}{N(t)|H|^{\frac{1}{2}}\lambda}} \right) \quad (30)$$

$$= 2 \exp \left( - \frac{\frac{1}{2}C^2 \log n}{C_1 + \frac{1}{3}C_2\xi} \right) \leq 2 \exp \left( - \frac{C_3 C^2 \log n}{1 + \xi} \right), \forall (\theta, t). \quad (31)$$

Therefore, if  $C_4 > 0$  is given, and we choose  $C^2 > \frac{3C_4}{C_3}$ , then we can write:

$$\sup_{(\theta, t) \in \mathbb{R}^p \times \mathcal{I}} \mathbb{P} \left( |\hat{p}(\theta, t) - \mathbb{E}[\hat{p}(\theta, t)|\mathcal{M}]| > C \left( \frac{\log n}{N(t)|H|^{\frac{1}{2}}\lambda} \right)^{\frac{1}{2}} \right) \leq 2 \exp \left( - \frac{3C_4 \log n}{1 + \xi} \right) \quad (32)$$

$$\leq 2n^{-\frac{3C_4}{1+\xi}}. \quad (33)$$

Now, letting  $\xi$  going to 0 we get:

$$\sup_{(\theta, t) \in \mathbb{R}^p \times \mathcal{I}} \mathbb{P}(|\hat{p}(\theta, t) - \mathbb{E}[\hat{p}(\theta, t)|\mathcal{M}]| > 0) \leq 2n^{-3C_4}. \quad (34)$$

Since we have that:

$$\begin{aligned} \sup_{(\theta, t) \in \mathbb{R}^p \times \mathcal{I}} \mathbb{P} \left( |\hat{p}(\theta, t) - \mathbb{E}[\hat{p}(\theta, t)|\mathcal{M}]| > C \left( \frac{\log n}{N(t)|H|^{\frac{1}{2}}\lambda} \right)^{\frac{1}{2}} \right) &\leq \\ \sup_{(\theta, t) \in \mathbb{R}^p \times \mathcal{I}} \mathbb{P}(|\hat{p}(\theta, t) - \mathbb{E}[\hat{p}(\theta, t)|\mathcal{M}]| > 0), &\end{aligned} \quad (35)$$

then:

$$\sup_{(\theta, t) \in \mathbb{R}^p \times \mathcal{I}} \mathbb{P} \left( |\hat{p}(\theta, t) - \mathbb{E}[\hat{p}(\theta, t)|\mathcal{M}]| > C \left( \frac{\log n}{N(t)|H|^{\frac{1}{2}}\lambda} \right)^{\frac{1}{2}} \right) = O(n^{-3C_4}). \quad (36)$$

Now restricting to finite subsets  $\mathcal{K}_n \subset \mathcal{K} \subset \mathbb{R}^p$  and  $\mathcal{I}_n \subset \mathcal{I}$  with at most  $O(n^{C_4})$  elements each, we have:

$$\mathbb{P} \left( \sup_{(\theta, t) \in \mathcal{K}_n \times \mathcal{I}_n} |\hat{p}(\theta, t) - \mathbb{E}[\hat{p}(\theta, t) | \mathcal{M}]| > C \left( \frac{\log n}{N(t) |H|^{\frac{1}{2}} \lambda} \right)^{\frac{1}{2}} \right) = O(n^{-C_4}). \quad (37)$$

From the Hölder-continuity of the kernels:

$$\begin{aligned} \sup_{(\theta, t) \in \mathcal{K} \times \mathcal{I}} \{ |\hat{p}(\theta, t) - \mathbb{E}[\hat{p}(\theta, t) | \mathcal{M}]| \} - D \|v^* - v_n^*\|^\alpha \leq \\ \sup_{(\theta, t) \in \mathcal{K}_n \times \mathcal{I}_n} |\hat{p}(\theta, t) - \mathbb{E}[\hat{p}(\theta, t) | \mathcal{M}]|, \end{aligned} \quad (38)$$

where

$$\begin{aligned} v^* &= \arg \sup_{(\theta, t) \in \mathcal{K} \times \mathcal{I}} |\hat{p}(\theta, t) - \mathbb{E}[\hat{p}(\theta, t) | \mathcal{M}]| \\ v_n^* &= \arg \sup_{(\theta, t) \in \mathcal{K}_n \times \mathcal{I}_n} |\hat{p}(\theta, t) - \mathbb{E}[\hat{p}(\theta, t) | \mathcal{M}]|, \end{aligned}$$

therefore:

$$\begin{aligned} \mathbb{P} \left( \sup_{(\theta, t) \in \mathcal{K} \times \mathcal{I}} |\hat{p}(\theta, t) - \mathbb{E}[\hat{p}(\theta, t) | \mathcal{M}]| > C \left( \frac{\log n}{N(t) |H|^{\frac{1}{2}} \lambda} \right)^{\frac{1}{2}} + D \|v^* - v_n^*\|^\alpha \right) \leq \\ \mathbb{P} \left( \sup_{(\theta, t) \in \mathcal{K}_n \times \mathcal{I}_n} |\hat{p}(\theta, t) - \mathbb{E}[\hat{p}(\theta, t) | \mathcal{M}]| > C \left( \frac{\log n}{N(t) |H|^{\frac{1}{2}} \lambda} \right)^{\frac{1}{2}} \right) \end{aligned} \quad (39)$$

now it is intuitive to show that  $\|v^* - v_n^*\| \leq \sqrt[p+1]{\frac{(K_{max} - K_{min})^p (I_{max} - I_{min})}{n^{2C_4}}}$ , where  $K_{max}$  e  $K_{min}$  are the endpoints for each dimension of  $\mathcal{K}$  (we assume them to be the same in each dimension for the sake of simplicity). Analogously for  $I_{max}$  and  $I_{min}$  (notice that  $\mathcal{I}$  is monodimensional).

Therefore:

$$\begin{aligned} \mathbb{P} \left( \sup_{(\theta, t) \in \mathcal{K} \times \mathcal{I}} |\hat{p}(\theta, t) - \mathbb{E}[\hat{p}(\theta, t) | \mathcal{M}]| > C \left( \frac{\log n}{N(t) |H|^{\frac{1}{2}} \lambda} \right)^{\frac{1}{2}} + \right. \\ \left. D \left( \frac{(K_{max} - K_{min})^p (I_{max} - I_{min})}{n^{2C_4}} \right)^{\frac{\alpha}{p+1}} \right) \leq \\ \mathbb{P} \left( \sup_{(\theta, t) \in \mathcal{K}_n \times \mathcal{I}_n} |\hat{p}(\theta, t) - \mathbb{E}[\hat{p}(\theta, t) | \mathcal{M}]| > C \left( \frac{\log n}{N(t) |H|^{\frac{1}{2}} \lambda} \right)^{\frac{1}{2}} \right). \end{aligned} \quad (40)$$

From (37) and (40), we can write:

$$\begin{aligned} \mathbb{P} \left( \sup_{(\theta, t) \in \mathcal{K} \times \mathcal{I}} |\hat{p}(\theta, t) - \mathbb{E}[\hat{p}(\theta, t) | \mathcal{M}]| < C \left( \frac{\log n}{N(t) |H|^{\frac{1}{2}} \lambda} \right)^{\frac{1}{2}} + \right. \\ \left. D \left( \frac{(K_{max} - K_{min})^p (I_{max} - I_{min})}{n^{2C_4}} \right)^{\frac{\alpha}{p+1}} \right) \geq 1 - O(n^{-C_4}) \end{aligned} \quad (41)$$

Therefore, as  $n \rightarrow \infty$  with probability 1:

$$\begin{aligned} |\hat{p}(\theta, t) - p(\theta, t) - O(\lambda) - O(\text{tr}(|H|))| = O \left[ \left( \frac{\log n}{N(t) |H|^{\frac{1}{2}} \lambda} \right)^{\frac{1}{2}} + \right. \\ \left. D \left( \frac{(K_{max} - K_{min})^p (I_{max} - I_{min})}{n^{2C_4}} \right)^{\frac{\alpha}{p+1}} \right], \forall (\theta, t) \in \mathcal{K} \times \mathcal{I} \end{aligned} \quad (42)$$

Finally, for a sufficiently large  $C_4$  from the above result we get:

$$\hat{p}(\theta, t) = p(\theta, t) + O \left[ \left( \frac{\log n}{N(t)|H|^{\frac{1}{2}}\lambda} \right)^{\frac{1}{2}} + \lambda + \text{tr}(H) \right], \forall (\theta, t) \in \mathcal{K} \times \mathcal{I} \quad (43)$$

□

## B Upper bound on the KL-Divergence between the prior and the posterior

In this section, we report the steps needed to get an upper bound on the KL-Divergence between the posterior  $q$  and the prior  $\hat{p}$ . Let us define  $S = \frac{1}{a_0(-\rho)N(t)\lambda} \sum_{t_i=\frac{1}{n}}^t \sum_{j=1}^{M_i} K_T(\frac{t-t_i}{\lambda})$ , hence:

$$D_{KL}(q||\hat{p}(\cdot, t)) = \int q(\theta) \log \frac{q(\theta)}{\hat{p}(\theta, t)} d\theta = \int q(\theta) \log \frac{q(\theta)}{\frac{S}{\hat{p}(\theta, t)}} d\theta \quad (44)$$

$$= \int q(\theta) \log \frac{q(\theta)}{\frac{1}{S a_0(-\rho)N(t)|H|^{\frac{1}{2}}\lambda} \sum_{t_i=\frac{1}{n}}^t K_T(\frac{t-t_i}{\lambda}) \sum_{j=1}^{M_i} K_S(H^{-\frac{1}{2}}(\theta - \theta_{ij}))} d\theta + \int q(\theta) \log \frac{1}{S} d\theta \quad (45)$$

Now the first term in Equation (45) is the KL-Divergence between two Mixture of Gaussians, which can be upper bounded using the same procedure as in [11], and the second term is a constant in the ELBO optimization. Therefore:

$$D_{KL}(q||\hat{p}(\cdot, t)) \leq D_{KL}(\chi^{(2)}||\chi^{(1)}) + \log \frac{1}{S} + \sum_{i,j} \chi_{j,i}^{(2)} D_{KL}(f_i^q||f_j^{\hat{p}}), \quad (46)$$

where we are rewriting  $q = \sum_i c_i^q f_i^q$  and  $\hat{p} = \sum_j c_j^{\hat{p}} f_j^{\hat{p}}$  with  $c_x^y$  being a generic weight and  $f_x^y = \mathcal{N}(\mu_x^y, \Sigma_x^y)$  being a generic component,  $(x, y) \in \{(i, q), (j, \hat{p})\}$ . Furthermore, we have:

$$\chi_{i,j}^{(1)} = \frac{c_j^{\hat{p}} \chi_{j,i}^{(2)}}{\sum_{i'} \chi_{j,i'}^{(2)}}, \quad \chi_{j,i}^{(2)} = \frac{c_i^{(q)} \chi_{i,j}^{(1)} e^{-D_{KL}(f_i^q||f_j^{\hat{p}})}}{\sum_{j'} \chi_{i,j'}^{(1)} e^{-D_{KL}(f_i^q||f_{j'}^{\hat{p}})}}. \quad (47)$$

Finally, notice that  $c_i^q = \frac{1}{C}$  for each  $i$ , where  $C$  is the number of components for the posterior, whereas  $c_j^{\hat{p}} = \frac{1}{S a_0(-\rho)N(t)\lambda} K_T(\frac{t-t_i}{\lambda})$ , with a little abuse of notation over the index  $i$  and  $j$ .

## C Proof of Theorem 4.1

The proof of Theorem 4.1 is straightforward, we just need to follow the same procedure of [35] plugging in the bound on the KL-Divergence of Equation 46. In the following we report the proof for completeness.

*Proof.* We start from Lemma 2 of [35] with variational parameter  $\hat{\xi} = (\hat{\mu}_1, \dots, \hat{\mu}_C, \hat{\Sigma}_1, \dots, \hat{\Sigma}_C)$ , whereas, for the right-hand side, we set  $\mu_i = \theta^*$  and  $\Sigma_i = cI$  for each  $i = 1, \dots, C$ , for some  $c > 0$ :

$$\begin{aligned} \mathbb{E}_{q_{\hat{\xi}}} \left[ \left\| \tilde{B}_{\theta} \right\|_{\nu}^2 \right] &\leq \inf_{\xi \in \Xi} \left\{ \mathbb{E}_{q_{\xi}} \left[ \left\| \tilde{B}_{\theta} \right\|_{\nu}^2 \right] + \mathbb{E}_{q_{\xi}} [v(\theta)] + 2 \frac{\psi}{N} D_{KL}(q_{\xi}||\hat{p}) \right\} + 8 \frac{R_{max}^2}{(1-\gamma)^2} \sqrt{\frac{\log \frac{2}{\delta}}{2N}} \\ &\leq \mathbb{E}_{\mathcal{N}(\theta^*, cI)} \left[ \left\| \tilde{B}_{\theta} \right\|_{\nu}^2 \right] + \mathbb{E}_{\mathcal{N}(\theta^*, cI)} [v(\theta)] + 2 \frac{\psi}{N} D_{KL}(\mathcal{N}(\theta^*, cI)||\hat{p}) + \\ &\quad 8 \frac{R_{max}^2}{(1-\gamma)^2} \sqrt{\frac{\log \frac{2}{\delta}}{2N}}. \end{aligned} \quad (48)$$



From Appendix B we have:

$$D_{KL}(\mathcal{N}(\theta^*, cI) \|\hat{p}) \leq D_{KL}(\chi^{(2)} \|\chi^{(1)}) + \log \frac{1}{S} + \sum_j \chi_j^{(2)} D_{KL}(\mathcal{N}(\theta^*, cI) \|\mathcal{N}(\theta_j, \sigma^2 I)), \quad (49)$$

where

$$\chi_j^{(1)} = c_j^{\hat{p}}, \quad \chi_j^{(2)} = \frac{c_j^{\hat{p}} e^{-D_{KL}(\mathcal{N}(\theta^*, cI) \|\mathcal{N}(\theta_j, \sigma^2 I))}}{\sum_{j'} c_{j'}^{\hat{p}} e^{-D_{KL}(\mathcal{N}(\theta^*, cI) \|\mathcal{N}(\theta_{j'}, \sigma^2 I))}} \quad (50)$$

obtained noticing that we can remove the index  $i$  because we have reduced the posterior to one component.  $\chi_j^{(2)}$  can be rewritten:

$$\chi_j^{(2)} = \frac{c_j^{\hat{p}} e^{-\frac{1}{2\sigma^2} \|\theta^* - \theta_j\|^2}}{\sum_{j'} c_{j'}^{\hat{p}} e^{-\frac{1}{2\sigma^2} \|\theta^* - \theta_{j'}\|^2}} \quad (51)$$

if we plug in the closed form expression of the KL-Divergence (52) into its definition.

$$D_{KL}(\mathcal{N}(\theta^*, cI) \|\mathcal{N}(\theta_j, \sigma^2 I)) = \frac{1}{2} \left( p \log \frac{\sigma^2}{c} + p \frac{c}{\sigma^2} + \frac{\|\theta^* - \theta_j\|^2}{\sigma^2} - p \right). \quad (52)$$

Now we proceed upper bounding the first and then the third term of 49:

$$D_{KL}(\chi^{(2)} \|\chi^{(1)}) = \sum_j \chi_j^{(2)} \log \frac{\chi_j^{(2)}}{\chi_j^{(1)}} \quad (53)$$

$$= \sum_j \chi_j^{(2)} \log \chi_j^{(2)} - \sum_j \chi_j^{(2)} \log \chi_j^{(1)} \quad (54)$$

$$\leq \sum_j \chi_j^{(2)} \log \frac{1}{c_j^{\hat{p}}} \quad (55)$$

where we got 55 just noticing in 54 that the first term is negative. Considering the third term, we have:

$$\begin{aligned} \sum_j \chi_j^{(2)} D_{KL}(\mathcal{N}(\theta^*, cI) \|\mathcal{N}(\theta_j, \sigma^2 I)) &= \frac{1}{2} \sum_j \chi_j^{(2)} \left( p \log \frac{\sigma^2}{c} + p \frac{c}{\sigma^2} + \frac{\|\theta^* - \theta_j\|^2}{\sigma^2} - p \right) \\ &\leq \frac{1}{2} p \log \frac{\sigma^2}{c} + \frac{1}{2} p \frac{c}{\sigma^2} + \sum_j \chi_j^{(2)} \frac{\|\theta^* - \theta_j\|^2}{2\sigma^2}. \end{aligned} \quad (56)$$

Therefore:

$$D_{KL}(\mathcal{N}(\theta^*, cI) \|\hat{p}) \leq \sum_j \chi_j^{(2)} \log \frac{1}{c_j^{\hat{p}}} + \log \frac{1}{S} + \frac{1}{2} p \log \frac{\sigma^2}{c} + \frac{1}{2} p \frac{c}{\sigma^2} + \sum_j \chi_j^{(2)} \frac{\|\theta^* - \theta_j\|^2}{2\sigma^2}. \quad (57)$$

Now leveraging the above equation, the following upper bound obtained in the proof of Theorem 3 in [35]:

$$\mathbb{E}_{\mathcal{N}(\theta^*, cI)} \left[ \left\| \tilde{B}_\theta \right\|_\nu^2 \right] \leq 2 \left\| \tilde{B}_{\theta^*} \right\|_\nu^2 + \frac{1}{2} \gamma^2 \kappa^2 c^2 \phi_{max}^4 + c(\theta_{max} \phi_{max} (1 + \gamma))^2, \quad (58)$$

and setting  $c = \frac{1}{N}$  (since the bound hold for any constant parameter  $c > 0$ ),  $c_1 = \frac{8R_{max}^2}{\sqrt{2}(1-\gamma)^2}$ ,  $c_2 = \theta_{max}^2 \phi_{max}^2 (1 - \gamma)^2 + \psi p \log \sigma^2 + 2\psi \sum_j \chi_j^{(2)} \log \frac{1}{c_j^{\hat{p}}} + 2\psi \log \frac{1}{S}$ ,  $c_3 = \frac{1}{2} \gamma^2 \kappa^2 \phi_{max}^4 + \frac{\psi p}{\sigma^2}$  and  $\varphi(\Theta_s) = \frac{1}{\sigma^2} \sum_j \chi_j^{(2)} \|\theta^* - \theta_j\|^2$ , we can rewrite Equation (48) in the following way:

$$\mathbb{E}_{q_\xi} \left[ \left\| \tilde{B}_\theta \right\|_\nu^2 \right] \leq 2 \left\| \tilde{B}_{\theta^*} \right\|_\nu^2 + v(\theta^*) + c_1 \sqrt{\frac{\log \frac{2}{\delta}}{N}} + \frac{c_2 + \psi p \log N + \psi \varphi(\Theta_s)}{N} + \frac{c_3}{N} \quad (59)$$

□

## D Experimental Details

In this section, we provide some additional experimental details together with further results.

### D.1 Parametrization

ADAM [14] is used in every experiment as optimizer. The source tasks are solved by a direct minimization of the TD error as described in section 3.4 of [35], using a *batch size* of 50 for the rooms environments and of 32 for Mountain Car, a *buffer size* of 50000, the projection parameter of the mellow-max TD error gradient set to 0.5, the learning rate  $\alpha = 10^{-3}$ . The exploration is  $\epsilon$ -greedy with  $\epsilon$  linearly decaying from 1 to 0.01 for Mountain Car and to 0.02 for the rooms environments. Both decays happens within 50% of the maximum number of learning iterations.

In the **rooms** environments, for what concern the two transfer algorithms, *c*-T2VT and *c*-MGVT, we have the following parametrization: *batch size* of 50, *buffer size* of 50000, projection parameter of the mellow-max TD error gradient set to 0.5 (see section 3.4 of [35]), the parameter of Equation (2)  $\psi = 10^{-6}$ , 10 weights to estimate the expected TD error, the learning rates are set to  $\alpha_\mu = 10^{-3}$  and  $\alpha_L = 0.1$  for the mean and the Cholesky factor  $L$  of the posterior (moreover, the minimum eigenvalue reachable by  $L$  is set to  $\sigma_{min}^2 = 10^{-4}$ ). Finally, for the prior, we use a diagonal isotropic matrix  $H = 10^{-5}I$  and  $\lambda = 0.3333$  in the context of *c*-T2VT, furthermore, we have  $\Sigma = 10^{-5}I$  for the prior in the context of *c*-MGVT.

In the **Mountain Car** environment, *c*-T2VT and *c*-MGVT are parametrized in the following way: *batch size* of 500, *buffer size* of 10000, projection parameter of the mellow-max TD error gradient set to 0.5, the parameter of Equation (2)  $\psi = 10^{-4}$ , 10 weights to estimate the expected TD error, the learning rates are set to  $\alpha_\mu = 10^{-3}$  and  $\alpha_L = 10^{-4}$  for the mean and the Cholesky factor  $L$  of the posterior (moreover, the minimum eigenvalue reachable by  $L$  is set to  $\sigma_{min}^2 = 10^{-4}$ ). Finally, for the prior, we use a diagonal isotropic matrix  $H = 10^{-5}I$  and  $\lambda = 0.3333$  in the context of *c*-T2VT, furthermore, we have  $\Sigma = 10^{-5}I$  for the prior in the context of *c*-MGVT.

### D.2 Temporal Dynamics

In this section, we provide the analytical form of the different dynamics employed in our experiments. Notice that this dynamics need to be plugged into the mean of our Gaussian distribution from where we sample the parametrization defining the task (for the rooms environment we will sample the positions of the doors, whereas, for the Mountain Car environment, we will sample the starting speed).

- **Linear:**  $2t - 1$ ,  $t \in [0, 1]$ ;
- **Polynomial:**  $at^4 + bt^3 + ct^2 + dt + e$ ,  $t \in [0, 1]$  and  $a = -15.625$ ,  $b = 39.5833$ ,  $c = -31.875$ ,  $d = 9.91667$  and  $e = -1$ ;
- **Sinusoidal:**  $\sin(2\pi t)$ ,  $t \in [0, 1]$ .

In Figure 4, we report the graphical representation of the above analytical functions.

Now, given the range for a parameter  $[k_{min}, k_{max}]$ , a given dynamic will span over this interval in the following way:  $d(t) \frac{(k_{max} - k_{min})}{2} + \frac{(k_{max} + k_{min})}{2}$ . Finally, notice that,  $[k_{min}, k_{max}] = [0.001, 0.0015]$  for Mountain Car, whereas  $[k_{min}, k_{max}] = [0.7 + padding, 9.3 - padding]$  for the parameters of the rooms environments. The *padding* variable is 0 for the 2-rooms, whereas is 2 for the 3-rooms environments. This *padding* variable was necessary in the 3-rooms environments in order for the TD gradient algorithm to be able to solve the source tasks in every configuration of the two doors.

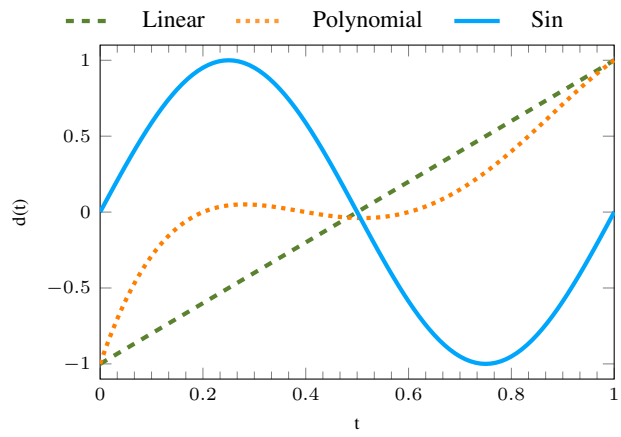


Figure 4: Temporal dynamics.